Supplement of

Characteristics and degradation of organic aerosols from cooking sources based on hourly observation of organic molecular markers in urban environment

*Correspondence: Li Li (Lily@shu.edu.cn)

Contents

Section S1. Observation instruments and factors

Hourly data for meteorological parameters, gaseous pollutants (NO_2 and O_3), $PM_{2.5}$ and its major chemical composition during the campaign were measured online. The meteorological parameters were obtained from a meteorological monitor (WXT520, VAISALA Inc., FL), which uses ultrasound to measure wind speed and direction, and a PTU module to measure atmospheric pressure, temperature and humidity using capacitive measurements; O_3 and NO_2 were measured by a ozone analyzer (49i-PS, Thermo Fisher Scientific, US) and NO_x (MODEL450i, Thermo Fisher Scientific, US) analyzer respectively; $PM_{2.5}$ mass concentration was measured by an online particulate matter monitor (BAM1020. Met One Inc., US) using the β-ray method; the concentration of the carbonaceous component of $PM_{2.5}$ was measured using a semi-continuous OC/EC analyzer (RT-4, Sunset Laboratory Inc, US) (Nicolosi et al., 2018; Zhang et al., 2017); ions and elements were measured by a MARGA ionic online analyzer (ADI2080, Metrohm, CHN) (Makkonen et al., 2012) and a atmospheric elements online monitor (EHM-X200, Tianrui, CHN).

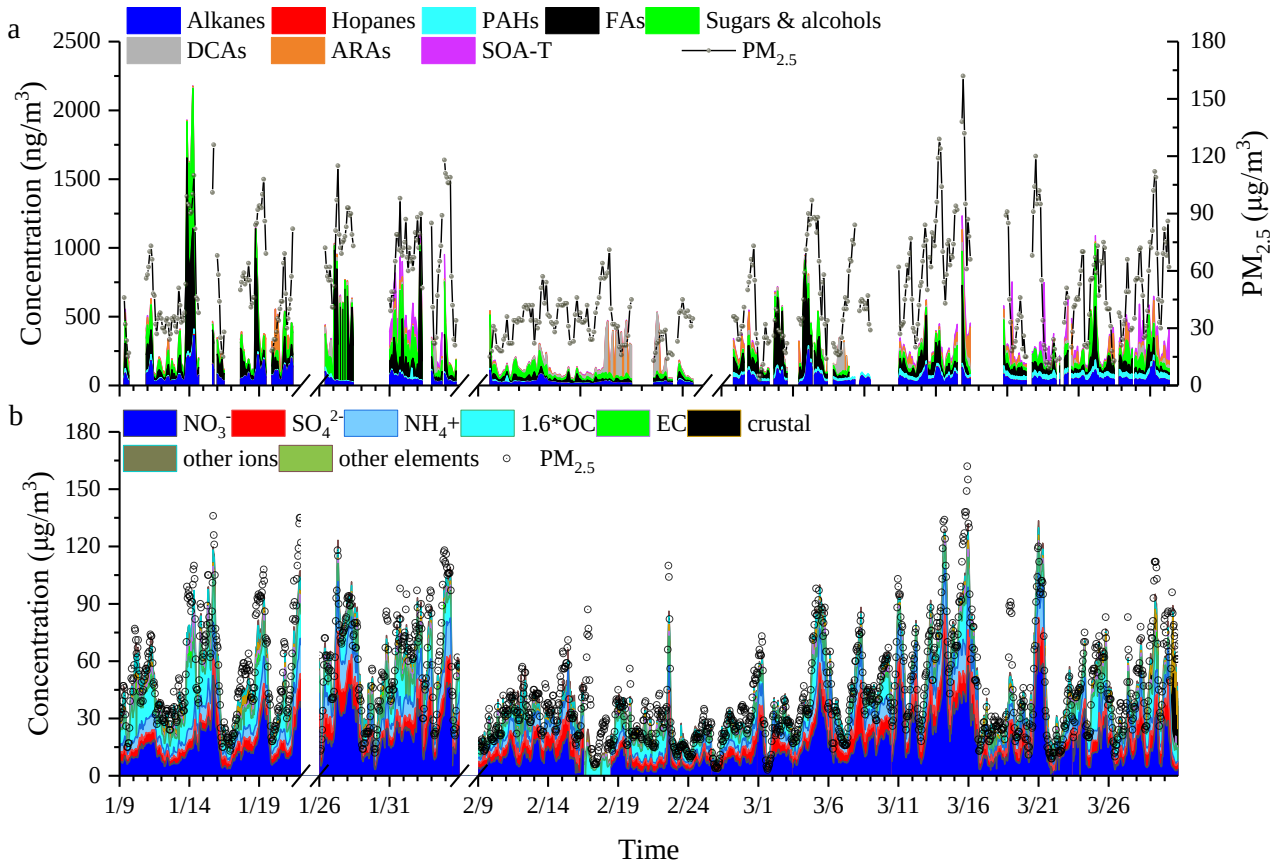

Figure S1. Time series of $PM_{2.5}$, chemical components and organic molecular tracers (PAHs, polycyclic aromatic hydrocarbons; DCAs, dicarboxylic acids; FAs, fatty acids; ARAs, aromatic acids; SOA-T, secondary organic aerosol tracers; crustal=2.20×[Al]+2.49×[Si]+1.63×[Ca]+2.42×[Fe]+1.94×[Ti] (Huang et al., 2014). **)**

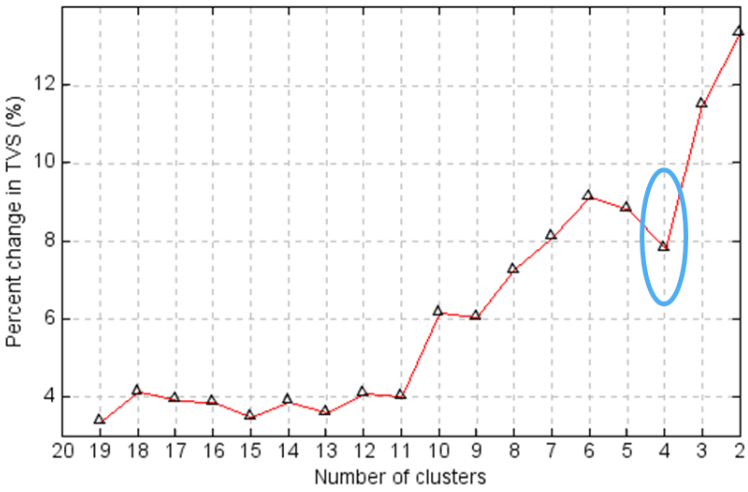

Figure S2. The variation of the total spatial variance (Choose the most appropriate clustering case based on the change in total spatial variance (TSV). The point raised down by TSV were selected as the optimal number of clusters, and the optimal solution of four clusters was finally extracted in this study (He et al., 2020).**)**

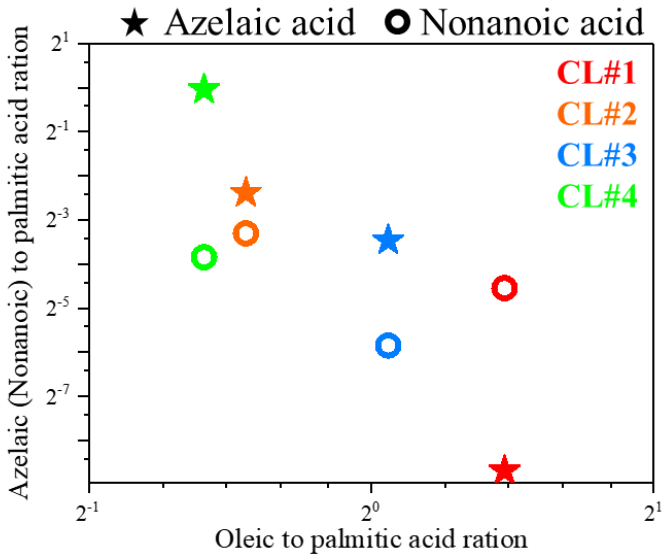

Figure S3. Correlation of Azelaic (Nonanoic) acid/palmitic acid ratio and oleic acid/palmitic acid ratio for the ambient samples

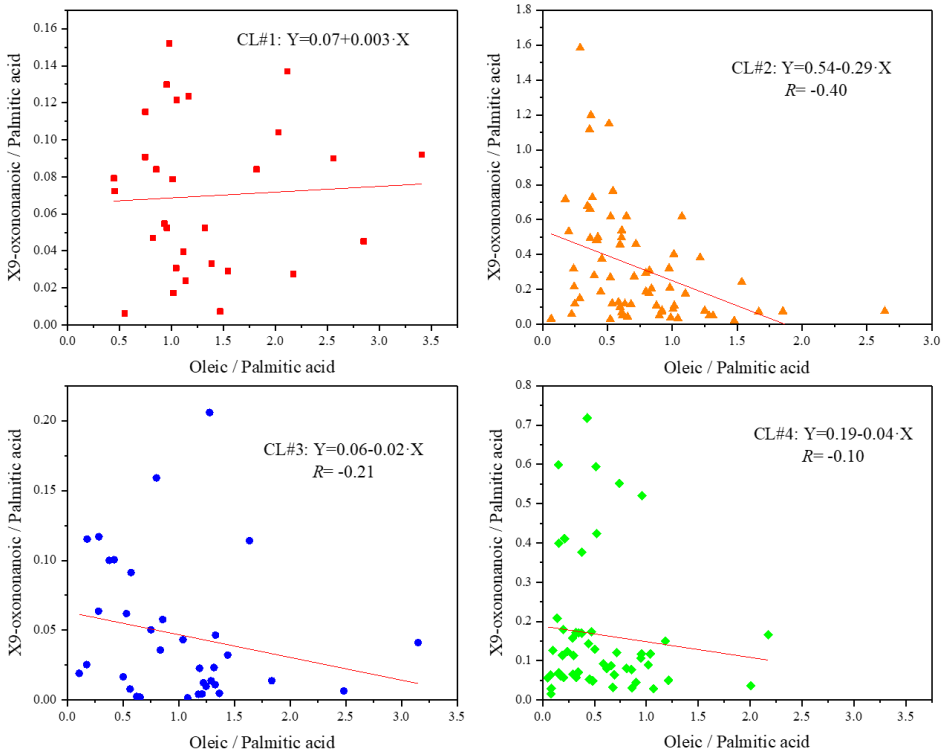

Figure S4. Correlation of X9-oxononanoic acid with oleic acid normalized by palmitic acid for the ambient samples under different sources of air masses

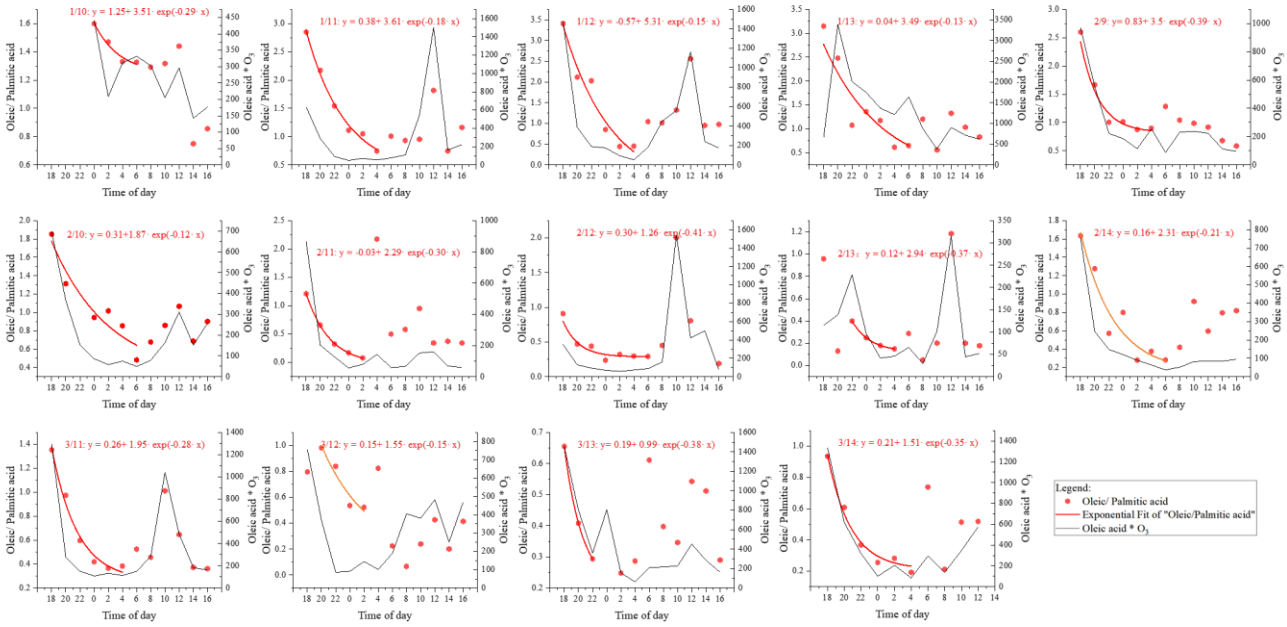

Figure S5. Day-to-day fitting of oleic acid normalized by palmitic acid

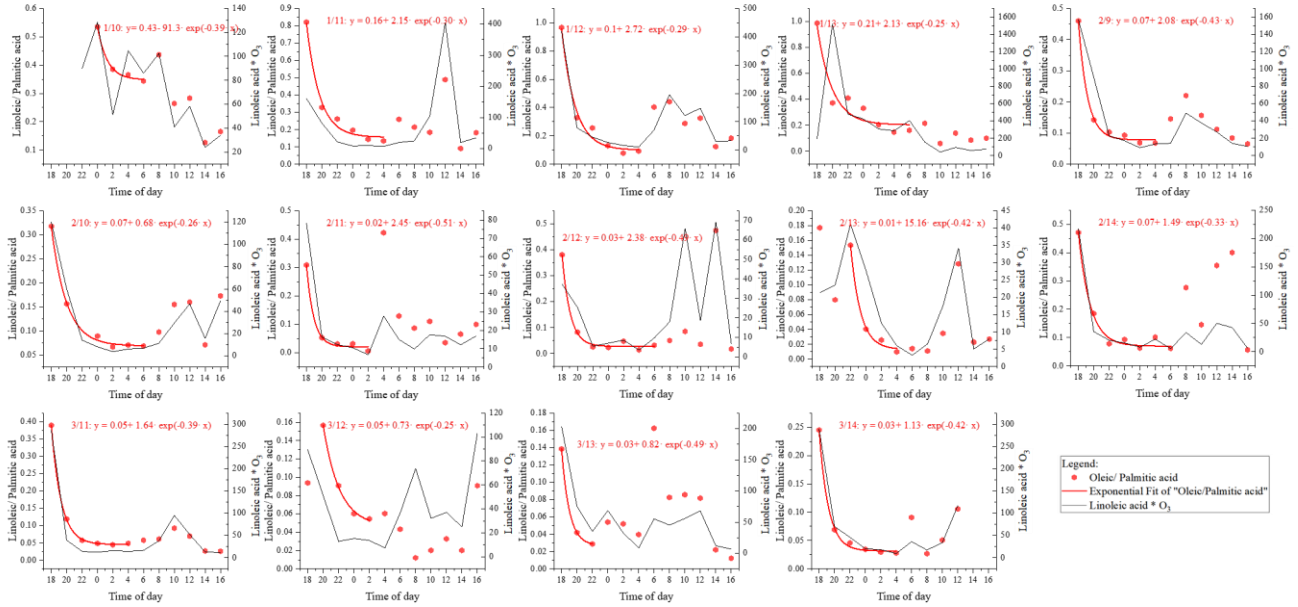

Figure S6. Day-to-day fitting of linoleic acid normalized by palmitic acid

Section S2. Source apportionment using PMF

Table S1 lists the input $PM_{2.5}$ and its components in the PMF modeling. The preferential input species for PMF are those with high abundance and source specific (Norris et al., 2014). Generally, organic markers with lower volatility and lower reactivity were selected. Figure S7(a) shows the PMF-resolved source profiles and time series of source contributions to OC for each source factor. Figure S7(b, c) shows the campaign-average percentage source contributions to OC and $PM_{2.5}$ from the PMF result (The time period is the whole observation period using TAG from January to March 2021, that is, the period of Figure S1). Here, we only briefly present the identification of each source factor.

A total of 10 factors are identified. Among them, seven are primary sources, they are industrial emission, biomass burning, vehicle exhaust, coal combustion, dust, cooking and fireworking. Three secondary sources, namely, secondary nitrate, secondary sulfate and SOA factor (Li et al., 2020; Wang et al., 2017).

Secondary nitrate factor is identified by high contributions of nitrate and ammonium. The secondary sulfate factor is characterized by high loadings of sulfate and ammonium. The SOA factor is characterized by high loadings of an anthropogenic SOA tracer (phthalic acid), isoprene SOA tracer (2-methylglyceric acid) and α-pinene SOA tracers (3-hydroxyglutaric acid, pinic acid and cis-pinonic acid) (Wang et al., 2017). The profile of industrial emission contains high loadings of Cr, Zn, Fe and Mn (Men et al., 2019; Pant and Harrison, 2013). Industry activities related to steel production, plating, and metallurgy often emit a large amount of these metallic elements. Biomass burning is identified by high loadings of levoglucosan and mannosan (Feng et al., 2013; Wang et al., 2019). The sixth factor contains a high

abundance of n-alkanes and hopanes, and is identified to be vehicle exhaust (Pant and Harrison, 2013; Wang et al., 2017). Coal combustion is identified by high loadings of Se, As and Pb (Chen et al., 2013; Wang et al., 2017), and the dust factor is distinguished by crustal elements (ions) Ca, Si, and Ti. The cooking factor is distinguished by fatty acids (oleic acid, palmitic acid and stearic acid) (Li et al., 2020). The fireworking factor is identified by high loadings of flammable metals such as Mg^{2+}, Cu and Ba, etc.

During the whole observation period with TAG, although the cooking factor contributes only a small fraction of $PM_{2.5}$ (4%), it accounts for 10.8% of the total OC, indicating the importance of cooking emissions to OM in the urban metropolis.

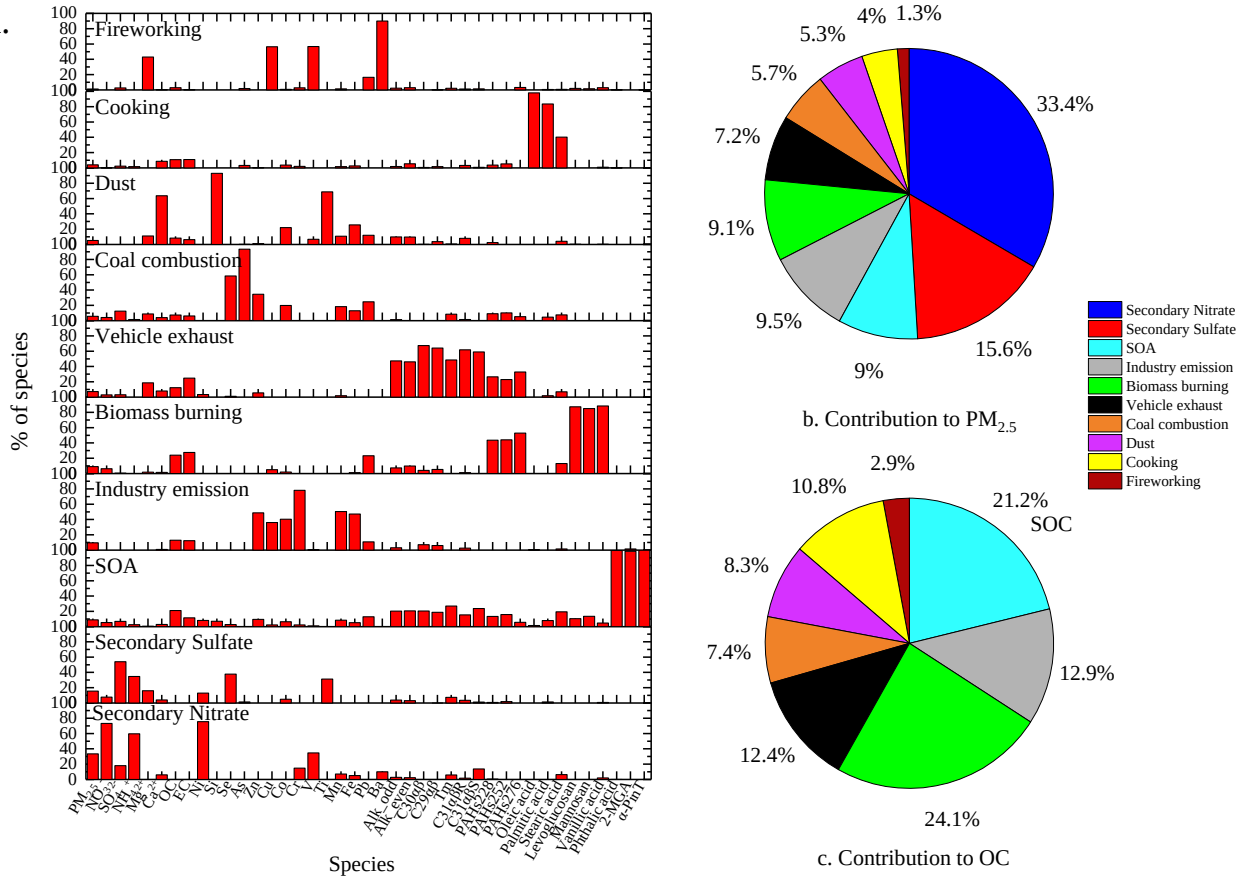

Figure S7. PMF resolved factor profiles (percentage of each species in each factor) (a); percentage contributions of individual factors to $PM_{2.5}$ (b) and to OC (c)

Table S1. $PM_{2.5}$ and its chemical components included in the PMF analysis

naming	grouping	unit	concentration
Alk_odd	*n*-C_{25}, *n*-C_{27}, *n*-C_{29}, *n*-C_{31} and *n*-C_{33}	ng/m^3	14.83
Alk_even	*n*-C_{24}, *n*-C_{26}, *n*-C_{28}, *n*-C_{30} and *n*-C_{32}	ng/m^3	17.65
C30αβ	17*α*(H)21*β*(H)-hopane	ng/m^3	0.27
C29αβ	17*α*(H)21*β*(H)-30-norhopane	ng/m^3	0.21
Tm	17*α*(H)-22,29,30-trisnorhopane	ng/m^3	0.1
C31αβR	17*α*(H)21*β*(H)-(22*R*)-homohopane	ng/m^3	0.1
C31αβS	17*α*(H)21*β*(H)-(22*S*)-homohopane	ng/m^3	0.17
PAHs228	Benzo[a]anthracene, Chrysene	ng/m^3	0.96
PAHs252	Benzo[b+k]fluoranthene, Benzo[a]pyrene	ng/m^3	1.44
PAHs276	Benzo[g,h,i]perylene, Indeno[1,2,3-cd]pyrene	ng/m^3	1.67
Oleic acid	Oleic acid	ng/m^3	28.09
Palmitic acid	Palmitic acid	ng/m^3	48.86
Stearic acid	Stearic acid	ng/m^3	19.94
Levoglucosan	Levoglucosan	ng/m^3	54.12
Mannosan	Mannosan	ng/m^3	4.23
Vanillic acid	Vanillic acid	ng/m^3	1.27
Phthalic acid	Phthalic acid	ng/m^3	16.71
2-MGA	2-Methylglyceric acid	ng/m^3	1.78
α-PinT	3-Hydroxyglutaric acid, Pinic acid, Cis-pinonic acid	ng/m^3	14.95
NO_3^-		μg/m^3	17.46
SO_4^{2-}		μg/m^3	7.50
NH_4^+		μg/m^3	7.59
Other ions	Mg^{2+}, Ca^{2+}	μg/m^3	0.46
OC		μg/m^3	5.98
EC		μg/m^3	1.87
Crustal elements	Si, Ti, Fe	μg/m^3	0.22
Other elements	Ni, Se, As, Zn, Cu, Co, Cr, V, Mn, Pb, Ba	μg/m^3	0.61
$PM_{2.5}$		μg/m^3	49.93
O_3		μg/m^3	49.09
NO_2		μg/m^3	45.27

References

Chen, J., Liu, G. J., Kang, Y., Wu, B., Sun, R. Y., Zhou, C. C., and Wu, D.: Atmospheric emissions of F, As, Se, Hg, and Sb from coal-fired power and heat generation in China, Chemosphere, 90(6), 1925-1932, doi:10.1016/j.chemosphere.2012.10.032, 2013.

Feng, J. L., Li, M., Zhang, P., Gong, S. Y., Zhong, M. A., Wu, M. H., Zheng, M., Chen, C. H., Wang, H. L., and Lou, S. R.: Investigation of the sources and seasonal variations of secondary organic aerosols in $PM_{2.5}$ in Shanghai with organic tracers, Atmos. Environ., 79, 614-622, doi:10.1016/j.atmosenv.2013.07.022, 2013.

He, X., Wang, Q. Q., Huang, X. H. H., Huang, D. D., Zhou, M., Qiao, L. P., Zhu, S. H., Ma, Y. G., Wang, H. L., Li, L., Huang, C., Xu, W., Worsnop, D. R., Goldstein, A. H., and Yu, J. Z.: Hourly measurements of organic molecular markers in urban Shanghai, China: Observation of enhanced formation of secondary organic aerosol during particulate matter episodic periods, Atmos. Environ., 240, doi: 10.1016/j.atmosenv.2020.117807, 2020.

Huang, X. H. H., Bian, Q. J., Ng, W. M., Louie, P. K. K., and Yu, J. Z.: Characterization of $PM_{2.5}$ Major Components and Source Investigation in Suburban Hong Kong: A One Year Monitoring Study, Aerosol Air Qual Res., 14(1), 237-250, doi:10.4209/aaqr.2013.01.0020, 2014.

Li, R., Wang, Q. Q., He, X., Zhu, S. H., Zhang, K., Duan, Y. S., Fu, Q. Y., Qiao, L. P., Wang, Y. J., Huang, L., Li, L., and Yu, J. Z.: Source apportionment of $PM_{2.5}$ in Shanghai based on hourly organic molecular markers and other source tracers, Atmos. Chem. Phys., 20(20), 12047-12061, doi:10.5194/acp-20-12047-2020, 2020.

Makkonen, U., Virkkula, A., Mantykentta, J., Hakola, H., Keronen, P., Vakkari, V., and Aalto, P. P.: Semi-continuous gas and inorganic aerosol measurements at a Finnish urban site: comparisons with filters, nitrogen in aerosol and gas phases, and aerosol acidity, Atmos. Chem. Phys., 12(12), 5617-5631, doi:10.5194/acp-12-5617-2012, 2012.

Men, C., Liu, R. M., Wang, Q. R., Guo, L. J., Miao, Y. X., and Shen, Z. Y.: Uncertainty analysis in source apportionment of heavy metals in road dust based on positive matrix factorization model and geographic information system, Sci. Total Environ., 652, 27-39, doi:10.1016/j.scitotenv.2018.10.212, 2019.

Nicolosi, E. M. G., Quincey, P., Font, A., and Fuller, G. W.: Light attenuation versus evolved carbon (AVEC) - A new way to look at elemental and organic carbon analysis, Atmos. Environ., 175, 145-153, doi:10.1016/j.atmosenv.2017.12.011, 2018.

Norris, G., Duvall, R., Brown, S., and Bai, S.: EPA positive matrix factorization (PMF) 5.0 fundamentals and user guide, U.S. Environmental Protection Agency, Washington, DC, EPA/600/R-14/108 (NTIS PB2015-105147), 2014.

Pant, P., and Harrison, R. M.: Estimation of the contribution of road traffic emissions to particulate matter concentrations from field measurements: A review, Atmos. Environ., 77, 78-97, doi:10.1016/j.atmosenv.2013.04.028, 2013.

Wang, Q. Q., He, X., Huang, X. H. H., Griffith, S. M., Feng, Y. M., Zhang, T., Zhang, Q. Y., Wu, D., and Yu, J. Z.: Impact of secondary organic aerosol tracers on tracer-based source apportionment of organic carbon and $PM_{2.5}$: A case study in the Pearl River Delta, China, Acs Earth Space Chem., 1(9), 562-571, doi:10.1021/acsearthspacechem.7b00088, 2017.

Wang, Q. Q., Huang, X. H. H., Tam, F. C. V., Zhang, X. X., Liu, K. M., Yeung, C., Feng, Y. M., Cheng, Y. Y., Wong, Y. K., Ng, W. M., Wu, C., Zhang, Q. Y., Zhang, T., Lau, N. T., Yuan, Z. B., Lau, A. K. H., and Yu, J. Z.: Source apportionment of fine particulate matter in Macao, China with and without organic tracers: A comparative study using positive matrix factorization, Atmos. Environ., 198, 183-193, doi:10.1016/j.atmosenv.2018.10.057, 2019.

Zhang, Q., Ning, Z., Shen, Z. X., Li, G. L., Zhang, J. K., Lei, Y. L., Xu, H. M., Sun, J., Zhang, L. M., Westerdahl, D., Gali, N. K., and Gong, X. S.: Variations of aerosol size distribution, chemical composition and optical properties from roadside to ambient environment: A case study in Hong Kong, China, Atmos. Environ., 166, 234-243, doi:10.1016/j.atmosenv.2017.07.030, 2017.